Value of proof load testing for prestressed concrete I-girder bridges in accordance with Eurocode-based safety levels

Addonizio, Gianmarco; Losanno, Daniele; Lantsoght, Eva O.L.; Casas, Joan R.

DOI
10.1016/j.engstruct.2025.121067

Publication date
2025

Document Version
Final published version

Published in
Engineering Structures

Engineering Structures 343 (2025) 121067

Contents lists available at ScienceDirect

Engineering Structures

journal homepage: www.elsevier.com/locate/engstruct

Value of proof load testing for prestressed concrete I-girder bridges in accordance with Eurocode-based safety levels

Gianmarco Addonizio [a,b,*], Daniele Losanno [a], Eva O.L. Lantsoght [c,d], Joan R. Casas [b]

[a] Department of Structures for Engineering and Architecture, University of Naples Federico II, Naples, Italy
[b] Department of Civil and Environmental Engineering, Universitat Politècnica de Catalunya, UPC-Barcelona-Tech, Barcelona, Spain
[c] Faculty of Civil Engineering and Geosciences, Delft University of Technology, Delft, the Netherlands
[d] College of Sciences and Engineering, Universidad San Francisco de Quito, Quito, Ecuador

ARTICLE INFO

Keywords:
Proof load testing
Existing bridges
Prestressed concrete
I-type girder
Structural reliability

ABSTRACT

Proof load testing (PLT) offers a valuable and sustainable alternative to analytical approaches for improving knowledge on the safety level of existing bridges, providing an in-situ measurement of structural bearing capacity under actual traffic loads by reducing resistance uncertainties and associated probability of failure if the test is passed. The present paper investigates the influence of the PLT on the structural reliability of prestressed concrete I-type simply-supported decks representing the most common type of existing bridges in Italy. By supplying data on the lower-bound of the capacity distribution, the PLT turns into an updated estimation of the bridge reliability. A fully-probabilistic analysis is developed combining random uncertainties on both materials and load effects with epistemic uncertainties. A traffic load model variable based on Eurocode Load Model 1 effects is calibrated to provide consistent modelling with code-prescribed safety levels. Structural capacity of the edge girder is considered both in terms of ultimate limit state for flexure and shear and serviceability limit state in terms of cracking load which could affect long-term bridge durability. The manuscript main contribution lies in developing a reliability-based approach to PLT that accounts for both prior (before test) and posterior (after test) structural reliability, incorporating conditioning on the success of the test. A sensitivity analysis according to the partial safety factor method is presented to investigate the impact of different proof loads assuming different Capacity-to-Demand Ratios (CDR). A case-study bridge is investigated where a proof load was executed recently demonstrating the benefit of the PLT in case of CDR lower than unit. The case study also showcases the possibility to significantly reduce the failure probability during the test when the target level is imposed with a number of intermediate levels of load steps.

1. Introduction

The management and safety assessment of ageing infrastructures have become critical global challenges, particularly in areas such as Europe, North America and some countries of South America [5,6,9,33], where the condition of existing infrastructures accounts for more than half-a-century operational life and the status of bridges is poor due to lack of maintenance and limited budget for maintenance. Therefore, the assessment of the actual structural capacity of existing bridges is a key point for the global asset management of transportation networks [25]. For instance, in Italy, a significant portion of the modern road network, spanning approximately 840,000 km, was constructed between 1955 and 1975 in simply supported configuration [31], resulting in an average frequency of one bridge every two kilometres along highways [29]. Additionally, the majority of the Italian road network (~80 %) is managed by municipalities and local authorities [4]. Similar considerations for ageing bridges can be made in the Netherlands and the United States [25].

This paper focuses on the potential impact of Proof Load Testing

Abbreviations: BRV, Basic Random Variable; CC, Consequence Class; CDF, Cumulative Density Function; CDR, Capacity-to-Demand Ratios; COV, Coefficient of Variation; FPM, Full Probabilistic Method; GRV, Geometrical Random Variables; HCPW, High Council of Public Works; LM1, Load Model 1 Eurocode; MBE, Manual for Bridge Evaluation; MCS, Monte Carlo Simulation; MRV, Material Random Variables; MTLE, Maxima Traffic Load Effects; MU, Model Uncertainty; PC, Prestressed Concrete; PDF, Probability Density Function; PMC, Probabilistic Model Code; PLT, Proof Load Test; PS, Prestressing Steel; PSFM, Partial Safety Factor Method; RS, Reinforcement Steel; SLS, Serviceability Limit State; ULS, Ultimate Limit State; WIM, Weigh-in-Motion.

* Corresponding author at: Department of Structures for Engineering and Architecture, University of Naples Federico II, Naples, Italy.
E-mail addresses: gianmarco.addonizio@unina.it, addoniziogianmarco@gmail.com (G. Addonizio).

https://doi.org/10.1016/j.engstruct.2025.121067
Received 10 April 2025; Received in revised form 22 July 2025; Accepted 28 July 2025
Available online 7 August 2025

List of symbols

A_{sp}	prestressing steel area
A_s	reinforcing steel area
e_c	traffic load eccentricity
EI	flexural stiffness
f_y	reinforcing steel conventional yield strength
$f_{p,01}$	prestressing steel conventional yield strength
G	dead and permanent load effect
$k^{(1)}$	primary torsional stiffness
$k^{(2)}$	secondary torsional stiffness
L	beam length
$m_x(x)$	uniformly distributed torque load
P_f	probability of failure
P	residual prestressing load
PL	proof load effect
Q_k^{LM1}	LM1 characteristic traffic load effect
R	resistance
S	first moment of area
TL	traffic load effect
z	beam distance from the deck centroid
α	proof load effect adimensionalized (over LM1 effect)
β	reliability index
Δl	total instantaneous and long-term prestressing losses
Δt	reference period
ϵ	torsion corrective factor
θ_i	model uncertainty
ξ	capacity sensitivity factor
σ_{0p}	initial prestressing stress
τ	traffic load distribution factor
$\varphi(x)$	torsional rotation angle
$\Phi(*)$	Gauss function
ψ	equivalent-tendon slope to the horizontal

(PLT), a complementary approach to numerical desk-study assessments which aims to assess the structural safety of bridges under external loads that are comparable to actual traffic actions and code-prescribed live loads. Target safety levels could be demonstrated by PLT as an alternative to both conventional (e.g. Partial Safety Factor Method PSFM) and unconventional (e.g. Full Probabilistic Method FPM) analytical methods once reliability-based proof-load design charts have been developed. PLT requires the application of a prescribed static loading protocol while monitoring the response of a bridge, therefore reducing uncertainty in resistance modelling and increasing the level of knowledge. PLT can be particularly valuable when conventional calculation techniques face limitations, such as the lack of original design documents [3,34] or when numerical and analytical models rely on simplifying assumptions or overconservative formulations. Even if a PLT may be more expensive than conventional safety checks performed according to a semi-probabilistic format with design values of loads and resistance obtained through partial safety factors, it should be considered that several local authorities have very limited level of knowledge and the number of bridges to be managed is very large thus a standardization of the PLT could be convenient. Globally, two primary approaches to PLT can be identified within existing code provisions. The first approach is outlined in the Manual for Bridge Evaluation (MBE) [1] and is common in the United States. This method prescribes a PLT to verify a bridge's capacity to sustain a "magnified" live load, i.e. a target load corresponding to a load-rating vehicle magnified by a factor in the range of [1.3–2.2] depending on a number of variables. In alternative approach, more common in Europe and particularly in Italy, a PLT is assumed as an "acceptance" load test, typically conducted after bridge construction or following major maintenance operations [15]. This acceptance test aims to ensure that the applied load yields an equivalent effect to the design unfactored (i.e. characteristic value) live load. However, the European framework for PLT remains fragmented, with considerable variability across codes and guidelines [25]. In 2020, the Italian High Council of Public Works (HCPW) issued new guidelines for classification and risk management, safety checks and monitoring of existing bridges [10,22]. The new guidelines introduced a "temporary operational" condition of the bridge, which could be demonstrated through load testing. Since the magnitude of the proof load is not based on reliability analysis and simplified magnification factors are proposed with respect to the load rating level, analytical safety checks have to be developed and completed within a period of 60 days from the test. In the United States, the calibration of proof load factors relies on previous studies such as [26,37] as cited in [1] and the more recent document [38]. In the European context, [7] proposed a methodology to calibrate proof loads for highway bridges based on available WIM (Weigh-in-Motion) data for traffic modelling, both in case original documents are available and unavailable. More recently, [11] suggested improvements to the MBE background documentation regarding PLT. However, when considering existing bridges before undertaking proof-loading or safety analysis, effects of *i*) climate change and scouring phenomena potentially affecting bridge foundations stability, *ii*) progressive corrosion of reinforcement and *iii*) fatigue damage should be duly considered as such hazards could undermine bridge residual capacity against traffic loads.

This study focuses on the application of PLT to prestressed concrete (PC) simply supported I-girder bridge type, exploring the correlation between prior and posterior reliability for future applications updating code provisions. A key objective of the research is to propose a general methodology for studying the potentialities and limitations of PLT assuming a Eurocode-conforming traffic load model in case WIM data is not made available. Indeed, the paper introduces a reliability-based PLT framework that quantifies structural safety both before and after testing by conditioning on a successful proof load. Proof load testing is investigated for safety analysis of ultimate limit state (ULS) failure modes of the edge girder in flexure and shear. An additional cracking limit state is introduced for damage control during the PLT considering the potential benefit of a conditional multi-step proof load. Two levels of analysis have been developed at the same time, i.e. semi-probabilistic according to partial safety factors method and fully probabilistic. Assuming different Capacity-to-Demand Ratios (CDR) in a partial safety factors format, the impact of the target proof load is evaluated both in terms of updated reliability levels after the execution of the PLT, and failure probability during the test considering material properties, self-weight and traffic load as random variables. A traffic load extreme value type distribution fitted on Eurocode LM1 [14] is provided to model a general traffic load independent on site-specific features, similar to what is proposed in [8,21]. In the second part of the paper, a real case study I-type PC bridge deck is investigated where a PLT has been recently conducted to demonstrate the usefulness of the methodology. This study showcases that PLT could be beneficial to those bridges with a CDR lower than unity, allowing to demonstrate adequate reliability levels and the extension of their service life.

2. Methodology for PLT

2.1. Flowchart of the methodology

This section presents the methodology developed within this study to investigate the impact of PLT on structural reliability of existing PC I-girder bridges as depicted by the flowchart in Fig. 1. Once the bridge has been selected, possible failure mechanisms should be considered according to structural design. Afterwards, a probabilistic characterisation of the basic independent random variables is required to perform a reliability analysis estimating the probability of failure before, during and after the PLT. To model the maximum traffic load effect within a given reference period, a Eurocode-based [14] probabilistic characterisation of the traffic load effect is proposed based on Load Model 1 (LM1). Failure mechanisms are considered in terms of nominal probability of exceeding limit states (LS) for flexure and shear (ULS) but also cracking condition at serviceability limit state (SLS). Target load effect PL_α is proposed in direct relationship with the load effect due to LM1 through a multiplication factor α, turning into a proof load effect PL_α equal to $\alpha \cdot LM1$. Acceptable α values are determined by combining a tolerable probability of failure during the test with a target reliability index to be attained after the PLT. At the end of the procedure the value of α should be selected from the set of possible values in order to perform a PLT which is consistent with imposed limitations. Benefit is conceived as increased reliability of the bridge in a specific reference period after the PLT, while the potential risk as the probability of damaging the structure during the PLT to be significantly limited.

Two levels of analysis were considered to assess structural safety according to a PSFM and FPM. Even if FPM requires statistical characterization and higher computational burden, it allows to explicitly account for the benefits of a PLT as an additional source of information when defining structural capacity. On the other hand, an estimate of the conventional safety level according to PSFM in terms of CDR can be valuable to better define the usefulness and the feasibility of a PLT in terms of increased reliability of the bridge together with the associated risk of damaging the structure.

The sensitivity of the PLT on CDRs will provide information on the effectiveness of the load test for real bridges. Reliability analyses are performed in MATLAB environment [36].

2.2. Bridge deck analysis & load effect models

In order to define load effects on I-type bridge decks, a grillage analysis model [20] was considered. In such a model external load with no transversal eccentricity (e.g. dead loads) generate bending moment and shear only in each girder according to the Bernoulli-Euler beam model. External loads that induce torsion can be distributed according to the general equation combining pure torsion and warping torsion:

$$k^{(2)} \cdot \varphi''''(x) - k^{(1)} \cdot \varphi''(x) = m_x(x) \tag{1}$$

with $\varphi(x)$ the torsional rotation angle of the beam with respect to its longitudinal axis x, $k^{(1)}$ and $k^{(2)}$ the primary and secondary torsional stiffness, respectively, $m_x(x)$ the external uniformly distributed torque load. In the case of I-girder bridges with a discrete number of transverse beams, the Engesser-Courbon method [32] can be adopted to calculate traffic load distribution factors τ_i among the different girders, i.e. neglecting pure torsion in each girder. Under this assumption, the transversal deflection profile of the deck is assumed to be linear and deck torsional stiffness is associated with the flexural stiffness of the girders only. Considering the flexural stiffness EI_i of the n girders equally spaced at distance z_i with traffic load having an eccentricity e_c from the central vertical axis of the deck, the load distribution factor of the i-th girder τ_i is:

$$\tau_i = \frac{EI_i}{\sum_{i=1}^{n} EI_i} + \frac{EI_i \cdot z_i}{\sum_{i=1}^{n} EI_i \cdot z_i^2} e_c \tag{2}$$

In case a corrective factor $\epsilon < 1$ is introduced to consider the contribution of primary torsional stiffness and the n deck girders having the same geometry, τ_i becomes:

$$\tau_i(\epsilon) = \frac{1}{n} + \epsilon \cdot \frac{z_i}{\sum_i z_i^2} e_c \tag{3}$$

where ϵ would be the ratio between rotation $\varphi(x)$ calculated by solving in a rigorous manner Eq. (1) and calculated under the assumption of pure secondary torsion according to the Engesser-Courbon method, respectively. It is proven that in the case of I-deck bridge decks with span no longer than 40 m and deck width larger than 9 m, this ratio typically falls between 0.85 and 0.95 [32]. Additionally, this coefficient can be experimentally calibrated through an in-situ load test measuring vertical displacement profile across the deck and girder strains. For the demand load effect both permanent G and traffic load TL were considered. The former was computed as a uniform load acting on each girder, being the overall transversal eccentricity of the deck and non-structural elements self-weight equal to zero. Traffic load will be imposed according to LM1 providing the characteristic value Q_k^{LM1} in terms of tandem and uniformly distributed loads to be applied to conventional lanes.

2.3. Capacity models

Structural capacity was analysed at the sectional level, defining sectional capacity model according to structural design principles and code provisions. As proposed by [28], the structural member strength R can be represented by the following expression:

$$R = f(\theta, GRV, MRV) \tag{4}$$

with MRV and GRV vectors of Material and Geometrical Random Variables, respectively, and θ the Model Uncertainties (MU) for the prediction of actual strength with deterministic mathematical models. This study assumed that mechanical properties do not change in space and time, thus randomness was only attributed to the original production process of each constitutive material due to the lack of informative data to generate random fields accounting for spatial and temporal variability. Materials of the same class, such as concrete, reinforcing and prestressing steel, were considered to be modelled with the same variable for the cross section under investigation. For example, the prestressing steel strength in the middle-span cross section was modelled with the same random variable for all strands. The deterioration process of materials and concrete strength increase over time were not explicitly included.

2.3.1. Prestressing load effect

The internal prestressing plays an important role on the capacity of PC girders both in service conditions and in shear resisting mechanisms [2]. The residual prestressing load P was modelled as a random variable composed of two components P_x and P_y in horizontal and vertical directions, respectively:

$$P_x(x/L) = \cos(\psi(x/L)) \cdot (1 - \Delta l) \cdot \sigma_{0p} A_{sp} \tag{5}$$

$$P_y(x/L) = \sin(\psi(x/L)) \cdot (1 - \Delta l) \cdot \sigma_{0p} A_{sp} \tag{6}$$

where $\psi(x/L)$ is the equivalent-tendon slope to the horizontal, L the beam length, Δl the total instantaneous and long-term prestressing losses (in %), σ_{0p} the initial prestressing stress, A_{sp} the total area of the strands.

2.3.2. ULS – flexure

The ULS resisting bending moment M_R of a PC girder can be evaluated through the following simplified relationship:

$$M_R = 0.9 d_s A_s f_y + 0.9 d_{sp} A_{sp} f_{p,01} \tag{7}$$

with A_s the reinforcement area of ordinary steel, $0.9d_s$ and $0.9d_{sp}$ the reinforcement and prestressing steel lever arms, f_y and $f_{p,01}$ the yield strength of ordinary reinforcement and strands, respectively. Basic as-

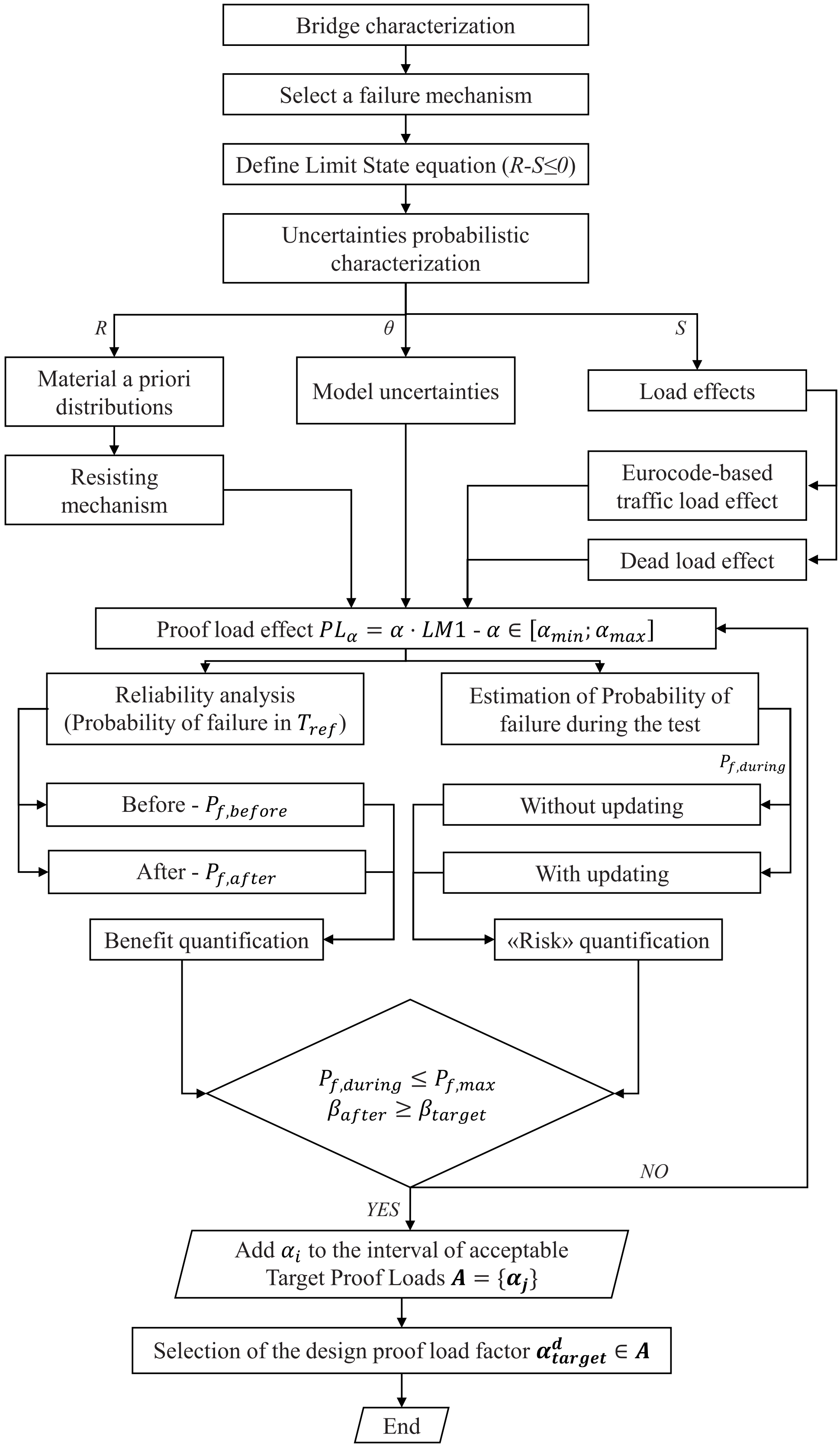

Fig. 1. Flowchart of the methodology to design PLT.

sumptions of Eq. (7) involve steel reinforcement lumped at its centroid, elastic-perfectly plastic constitutive model for both ordinary and prestressing steel; concrete crushing in compression and yielded reinforcement due to the relatively low reinforcement ratio, i.e. at ULS strands always yielded even discarding residual prestressing strain as initial value. This assumption is supported by previous studies on a class of simply supported I-type existing bridge decks [29,30] where reinforcement ratios not significantly higher than 1 % were reported turning into ductile flexural failure mechanism. In the adopted formulation, the influence of the reinforcement in the compression zone is not considered due to limited contribution in bending. In future studies, more refined sectional models could take into account variability in lever arm estimation and the inherent uncertainties associated with strain compatibility assumption (e.g. in case of unbonded or external post-tensioning).

2.3.3. ULS – shear

For the evaluation of the shear capacity V_R of a PC girder three different capacity models were considered according to Eurocode 2 [15]:

- Beams in uncracked configuration (i.e. shear-tension failure mode):

$$V_{R,U} = \frac{I}{S} b_w \sqrt{f_{ct}^2 + f_{ct}\sigma_{cp}} \tag{8}$$

- Beams with transverse shear reinforcement (i.e. truss model):

$$V_{R,T} = \min\left(V_{R,S}; V_{R,C}\right) \tag{9}$$

$$V_{R,S} = \frac{A_{sw}}{s} z \cdot f_{yw} \cdot \cot(\theta) \tag{10}$$

$$V_{R,C} = 0.5 b_w z \cdot \alpha_{cw} f_c \cdot \frac{1}{\cot(\theta) + \tan(\theta)} \tag{11}$$

- Beams without shear reinforcement (i.e. flexure-shear capacity)

$$V_{R,WS} = \left[C_{Rd,c} k (100 \rho f_{ck})^{1/3} + k_1 \sigma_{cp}\right] \cdot b_w d \tag{12}$$

The maximum value between the three formulations was considered to provide the actual shear capacity of the girder, provided that in case $V_R = V_{R,U}$ the cross section is uncracked due to external bending moment:

$$V_R = \max(V_{R,U}; V_{R,T}; V_{R,WS}) \tag{13}$$

In Eq. (8) the ratio between the inertia moment and static moment I/S was considered equal to $0.7d$ according to the Italian National Code [23], where d is the total height of the cross section reduced by the concrete cover. When calculating internal shear force, the beneficial contribution of prestressing was also taken into account and set equal to $P_y(x/L)$.

2.3.4. SLS – cracking

A cracking limit state was considered both to study the probability of damaging the structure during the PLT and to increase the level of knowledge about tensile concrete strength and residual prestressing random variables. Unlike ultimate limit states, cracking is significantly influenced by the staged construction process. For this reason, the bottom fibre stress of the I-girder was evaluated considering the different construction stages (m in total) which occurred at different times and compared to the estimated concrete tensile strength f_{ct}. The external traffic load effect M_{TL} can be compared with the cracking moment $M_{CR}(x)$ defined as:

$$M_{CR}(x) = \frac{I_m}{y_m^c} \cdot \left[f_{ct} + \sum_{i=1}^{m} \left[\frac{P_{x,i}(x)}{A_i} + \frac{P_{x,i}(x)\, e_i(x) - M_{G,i}(x)}{I_i} y_i^c \right] \right] \tag{14}$$

with y_i^c the distance between the centroid and the bottom concrete fiber at the i-th stage, $e_i(x)$ the equivalent-tendon eccentricity with respect to the section centroid at the i-th stage, f_{ct} the tensile concrete strength and $M_{G,i}$ the permanent load effect during the i-th construction stage.

2.4. Partial safety factor method

PSFM is widely adopted in common engineering practice for structural design, where uncertainties are indirectly taken into account through properly calibrated partial safety factors. In general, design values of load effect (E_d) and resistance (R_d) are obtained by imposing partial safety factors to the characteristic values (F_k,X_k) of both loads and materials. Simplified relationships between partial safety factors γ_i and the Basic Random Variables (BRV) are the following:

$$E_d = E\left[\gamma_{F,i} \cdot \psi F_k\right] \tag{15}$$

$$R_d = R\left[\frac{X_{k,i}}{\gamma_{M,i}}\right] \tag{16}$$

with F_k the characteristic value of the action; $\psi = \{1, \psi_0, \psi_1, \psi_2\}$ a factor to obtain the representative value of the action for combinations of loads; $\gamma_{F,i}$ and $\gamma_{M,i}$ are the load effect and resistance safety factor, respectively.

For the three limit states under consideration (ultimate flexural capacity, ultimate shear capacity, flexural cracking), according to PSFM the corresponding CDR were defined as the ratio between the design capacity and the corresponding demand for each mechanism:

$$CDR(\xi_F) = \frac{M_{Rd}}{M_{Sd}} = \frac{\xi_F \cdot \left[0.9 d_s A_s f_{y,k} / \gamma_s + 0.9 d_{sp} A_{sp} f_{p,01,k} / \gamma_s\right]}{\gamma_G M_{G,k} + \gamma_{TL} M_{TL,k}} \tag{17}$$

$$CDR(\xi_V) = \frac{V_{Rd}}{V_{Sd}} = \frac{\xi_V \cdot V_R(\gamma_C; \gamma_S)}{\gamma_G V_{G,k} + \gamma_{TL} V_{TL,k} - \gamma_P V_P} \tag{18}$$

$$CDR(\xi_{CR}) = \frac{\xi_{CR} \cdot M_{CR}}{M_{TL,f}} \tag{19}$$

where:

- γ_i are the partial safety factors;
- the subscript k indicates the characteristic value;
- the subscript d indicates the design value;
- $M_{TL,f}$ indicates the frequent value of the traffic load distribution;
- ξ_j is the capacity sensitivity factor, whose unit value provides the actual capacity for each mechanism.

The parameter ξ_j was introduced to investigate the sensitivity of the PLT on different safety levels and its effectiveness.

3. Reliability analysis for PLT

In contrast with PSFM, the FPM explicitly models different types of uncertainties adopting probability theory to estimate the failure probability P_f, which is the probability to exceed a considered limit state within a reference time period Δt. In this study, Monte Carlo Simulation (MCS) was adopted as analysis method generating a number of random samples N from the BRV in a range between 10^7 and $5 \cdot 10^9$ depending on expected reliability. In the following the reliability index β is computed according to the well-known relationship $P_f = \Phi(-\beta)$, with $\Phi(*)$ the cumulative distribution function (CDF) of the standard normal distribution.

3.1. Benefit of the PLT

Before performing any PLT, there is an intrinsic probability of failure as the probability of any specific limit state LS_j being exceeded in Δt. Such probability of failure was arbitrarily defined as "*before*":

$$P_{f,before}(LS_{j,0}, \Delta t) = P[LS_{j,0} \leq 0] \tag{20}$$

where

$$LS_{j,0} = \theta_R R_j - \theta_E (G + TL(\Delta t)) \tag{21}$$

with R_j the capacity associated with the failure mechanism j, G and TL the permanent and traffic load effects, θ_R and θ_E the MUs of the resistance and load effect variables.

A PLT can be seen in terms of additional information about structural resistance as it can increase the reliability of the structure in case of a positive outcome from the test. Generally, the proof load results in an updated probability of failure through either indirect or direct conditioning. The former method is based on updating the BRVs, such as, for example, concrete tensile strength or elastic modulus.

Alternately, the direct conditioning method considers only realizations for which no failure occurred during the PLT. This article assumed direct conditioning to update the original estimation of P_f. Therefore, the probability $P_{f,after}(LS_j, \Delta t, PL_\alpha)$, named as "*after*" or simply "*conditioned*", was conceived as the probability that a specific limit state LS_j associated with the failure mechanism j is exceeded in a fixed time period Δt, conditional to the success of the PLT having a target $PL_\alpha = \alpha \cdot LM1$:

$$P_{f,after}(LS_j, \Delta t, PL_\alpha) = P[LS_{j,0} \leq 0 \mid LS_{PL_\alpha} > 0] \tag{22}$$

where

$$LS_{PL_\alpha} = \theta_R R_j - \theta_E G - \theta_{PL} PL_\alpha \tag{23}$$

with θ_{PL} the proof load effect MU. A successfully completed PLT can be interpreted as the event of not exceeding the same limit state LS_{PL_α} during the test.

3.2. Probability of failure during the PLT

The limits of a PLT are basically related to the possibility of temporarily or permanently damaging the structure. A valuable tool for managing the potential risk during the execution of a PLT is the estimation of the probability of failure during the test $P_{f,during}$. $P_{f,during}$ can be defined as:

- Unconditioned failure probability, $P^u_{f,during}$, calculated without considering the step-by-step loading procedure usually imposed in a real test but only its target level PL_α:

$$P^u_{f,during}(LS_j, PL_\alpha) = P[LS_{PL_\alpha} \leq 0] \tag{24}$$

- Conditioned failure probability, $P^c_{f,during}$, calculated assuming an incremental loading protocol made of n loading steps up to the target load PL_α. In this case the probability of failure at the loading step i-th is based on the success of the $(i-1)$-th step, i.e. informed by the real-time absence of damage for the previous load effect.

$$P^c_{fi,during}(LS_j, PL_\alpha, i) = P[LS_{PL_i} \leq 0 \mid LS_{PL_{i-1}} > 0] \tag{25}$$

The unconditioned probability of cracking during the PLT was conceived as:

$$P^u_{CR}(LS_j, PL_\alpha) = P[LS_{CR} \leq 0] \tag{26}$$

where

$$LS_{CR} = M_{CR} - \theta_{PL} PL_\alpha \tag{27}$$

with M_{CR} the cracking moment defined in Eq. (14). Similarly to the conditioned probability of failure for ultimate limit states, a conditioned probability of cracking is defined as P^c_{CR} in order to consider different loading protocols.

3.3. Target reliability

Definition of target reliability for existing bridges should be framed in the lifetime period of the structure, performing risk-analysis for each case study. It is commonly acknowledged that target reliability of existing structures can be lower than for new ones. According to *fib* bulletin 80 [18], in this study two classes of reliability indexes for ULS will be considered as a function of the Consequence Class (CC) of the structure: β_0 for assessment and β_{up} for structural retrofit (Table 1). It can be assumed that highway bridges are in CC3 while most of roadway bridges can be classified in either CC2 or CC3. According to [24] irreversible SLS annual target reliability indexes depending on safety-measure cost vary in the range [1.3–2.3].

3.4. Random variables

FPM requires a statistical definition of the BRV affecting structural safety. Subsequently, the estimation of the BRV parameters and the choice of the probabilistic models would play a key role in deriving an accurate estimation of structural reliability. Among the different types and sources of uncertainties, in following analyses both physical and model uncertainties were considered. MU were conceived as the difference between the experimental observations and the predictions of the models adopted and were considered as random variables as suggested by [24] for load effects ($\theta_E; \theta_{PL}$) and resistance (θ_R). Physical uncertainty seeks to capture the intrinsic variability inherent in random variables, such as material properties and loads. Material properties can be obtained through prior knowledge of the structure and/or on laboratory tests. As already mentioned, the demand load effect is considered to be composed of a permanent and a traffic load effect, apart from the beneficial prestressing load directly acting on the girder. Uniformly distributed permanent load q_G acting on each girder was considered to model deck self-weight plus non-structural components. Uncertainties were related to weight density and dimensions of structural and non-structural members. According to the Probabilistic Model Code (PMC) [24], a Gaussian distribution can be assumed as random variable to model the permanent load effect G, consistently with relevant modelling assumptions in the field of PLT [7,12]. The mean value was assumed to be equal to the nominal value reported by original drawings confirmed by visual inspections. The coefficient of variation CoV_G was set equal to 5%. The traffic load model is discussed in the following section. Another relevant random variable is the proof load effect PL_α, modelled as a gaussian variable with mean μ_{PL_α} and coefficient of variation of $CoV_{PL_\alpha} = 5\%$. Particularly, the expected value was assumed to be equal to:

Table 1
50-yr ULS target reliability indexes [18].

Consequence Class	β_{up}	β_0
CC1	$3.3 - 0.5 = 2.8$	$3.3 - 1.5 = 1.8$
CC2	$3.8 - 0.5 = 3.3$	$3.8 - 1.5 = 2.3$
CC3	$4.3 - 0.5 = 3.8$	$4.3 - 1.5 = 2.8$

$$\mu_{PL_\alpha} = EV(PL_\alpha) = \alpha \cdot Q_k^{LM1} \tag{28}$$

with α a scalar number arbitrarily defined. The value of CoV_{PL_α} is justified by a strict and stepwise control of the imposed proof-load, its spatial location and reproduced effects. For example, test vehicles have to be weighted prior to test both in terms of total weight and axle-load distribution, while in case hydraulic jacks are used they can provide a continuous measure of the imposed load by means of load cells. In order to reduce CoV_{PL_α} to acceptable values load-test design would require in-depth knowledge of the load protocol and an accurate longitudinal and transverse positioning of the external load. Additionally, the initial load steps (before target is attained) aid in controlling load effect, since they can be explicitly used to validate the adopted structural model. Different assumptions were made in terms of loading steps of the loading protocol to achieve PL_α thus assuming unconditional to be compared with conditional probability when calculating $P_{f,during}$.

3.5. Eurocode-based traffic load model

The Eurocode [14] allows to compute the characteristic value Q_k^{LM1} defined as the traffic load effect with a 1000-year return period, i.e. having 5 % probability of exceedance in 50 years. Assuming to define a probabilistic characterization of the maxima traffic load effects (MTLE) in a specific time period, in this study three main assumptions were introduced:

- The characteristic value Q_k^{LM1} represents the k-th order quantile of MTLE in a specific time period;
- The Gumbel random variable model is considered appropriate to model the MTLE;
- The coefficient of variation CoV_{TL} of the MTLE was selected based on data from the literature on traffic load characterization.

The characteristic value Q_k^{LM1} can be computed through structural analysis by applying LM1 at the position that provides the most adverse load effects resulting from moving traffic lanes in both longitudinal and transverse directions. Assuming $TL \sim Y$, whose realizations are y, the Probability (PDF) and Cumulative (CDF) Density Function adopted for the Gumbel distribution with parameters (u,γ) are:

$$f_Y(y) = \gamma \cdot \exp[-\gamma(y-u) \; - \; e^{-\gamma(y-u)}] \tag{29}$$

$$F_Y(y) = \exp\left[-\exp^{-\gamma(y-u)}\right] \tag{30}$$

Imposing the following linear system, the traffic random variable TL was obtained accordingly:

$$\begin{cases} k = \exp\left[-e^{-\gamma\left(Q_k^{LM1}-u\right)}\right] \\ CoV_{TL} = \dfrac{\sigma_Y}{\mu_Y} = f(\gamma, u) \end{cases} \tag{31}$$

It is worth mentioning that this procedure is consistent with that suggested in [21], where the value of CoV_{TL} is considered dependent on the reference period assumed, i.e. equal to 7.5 % and 6.1 % in 1 and 50 years, respectively. The same document refers to the project ARCHES D08 [16], where actually measured coefficients of variation of annual maxima of traffic load are in the range $[3;15]$%. Fig. 2 shows the CDFs and PDFs of a Eurocode-based generic load effect Q_k^{LM1} (with unit of measurement UM) for three values of CoV_{TL} (5 %, 10 %, 15 %) and two reference periods (1 and 50 yrs). From these plots it can be noted how Q_k^{LM1} has the same exceedance probability for a given Δt. The larger the CoV_{TL}, the lower the mean value of the TL distribution. Moreover, the 50-year load maxima have a larger mean value than the 1-year ones, in accordance with the extreme value theory.

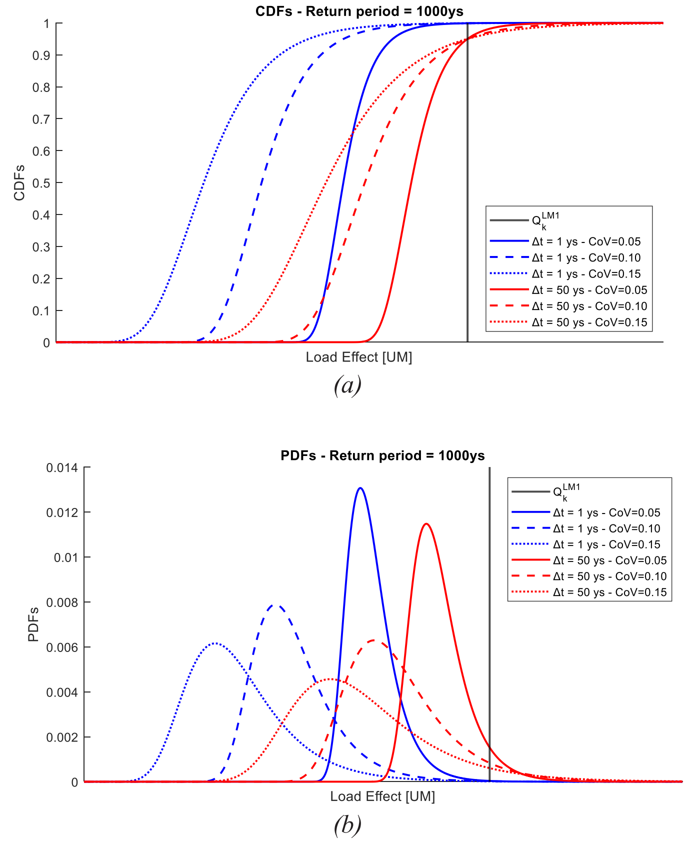

Fig. 2. CDF (a) and PDF (b) of Eurocode LM1-based Traffic Load Effect Distributions.

4. Case study bridge

4.1. Description of case study

A real case study was selected to investigate the impact of the PLT according to the proposed methodology. The illustrative example is an I-girder PC bridge built during the '60 s along an important highway in Southern Italy with two carriageways on two separate decks (Fig. 3).

With a span length of 42 m and a total length of around 900 m with 21 spans, the bridge deck is simply supported and it is composed of 3 m high PC I-girders, a concrete top slab (variable thickness between 0.20 and 0.30 m) and four transverse prestressed concrete beams (Fig. 4), two at the supports and two at 1/3 and 2/3 of the span length. In Fig. 4, a detailed transverse layout of strands and reinforcing steel is displayed for mid-span cross section. Fig. 5 shows the longitudinal layout of the strands on half girder for a total of 80 7-wire strands having 1/2" diameter.

Original design and retrofit plans were made available to the authors. An acceptance load test after retrofit interventions of the bridge was performed with a total of eight 42 t heavy trucks. The aim of the load test was to reproduce the maximum LM1 effects both in terms of bending moment at mid-span and shear at supports, computed through a linear FEM model of the deck. The structural response during the PLT was monitored demonstrating linear behaviour and no damage upon unloading with a fully reversible behavior. Distribution factors among beams were measured during the load test and validated in terms of vertical displacements and deck deflection.

Additionally, for the analysis of internal stress distribution in the midpsan cross section, two construction stages were considered corresponding to I-girder and a T-girder cross section, respectively:

Fig. 3. View of the case-study bridge (Google Maps).

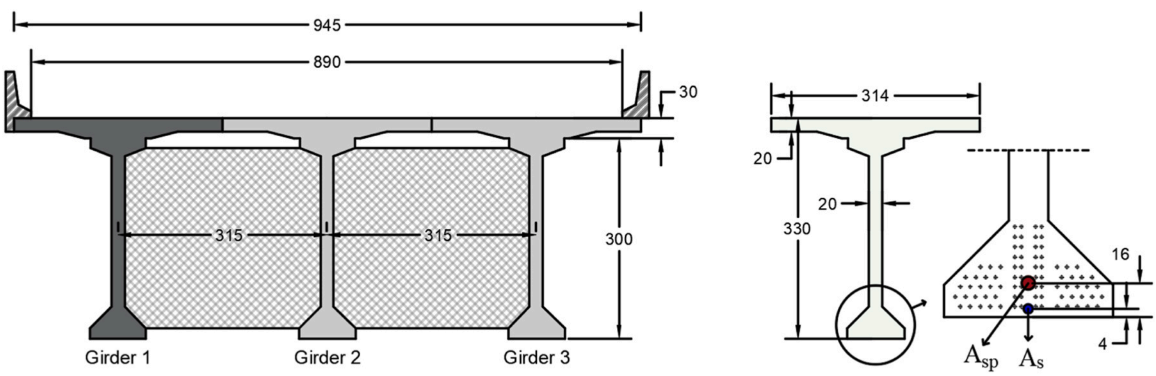

Fig. 4. Bridge Deck and Edge Girder Cross Sections at Midspan with equivalent reinforcement position A_{sp} and A_s (dimensions in cm).

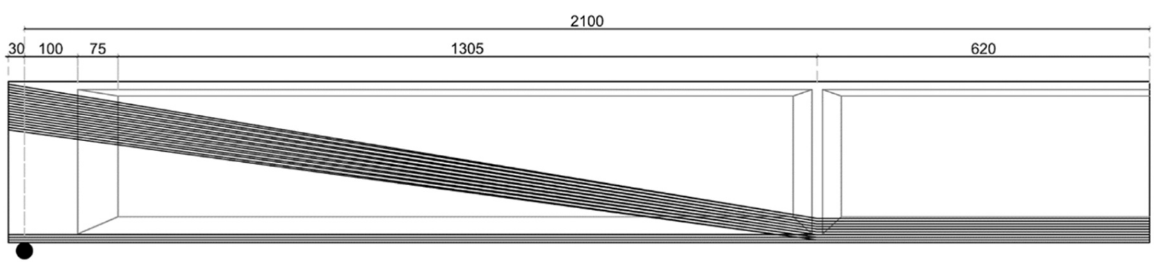

Fig. 5. Longitudinal strands layout of the half girder (dimensions in cm).

- Stage 1: girder casting, prestressing, slab casting (acting on the girder only)
- Stage 2: nonstructural elements and road pavement, traffic load, proof load (acting on the girder with top slab)

In Table 2 geometrical properties are reported and modelled as deterministic variables.

4.2. Model random variables

Materials properties have been defined in Table 3 in terms of prestressing steel (PS), reinforcement steel (RS) and concrete (C). Even if original drawings were available for all different materials, additional in-situ tests were performed for concrete compressive strength.

Additionally, the beneficial effect of prestressing $P_y(x = d)$ at the shear critical position d was modelled as a lognormal random variable with $EV(P_y) = 505kN$ and $CoV_{P_y} = 4.5\%$.

4.3. Capacity

The undamaged bending resisting moment M_R at midspan was modelled as normal random variable $N(38MNm, 0.89MNm)$ being a linear combination of independent gaussian random variables, $f_{p,01}$ and f_y. Assuming μ_{M_R} and σ_{M_R} the resistance mean and standard deviation, respectively, the capacity sensitivity factor ξ_F was defined as:

$$M_R(\xi_F) = N\left(\xi_F \cdot \mu_{M_R}\ ;\ \sigma_{M_R}\right)$$

with $\xi_F = [1.00 - 0.95 - 0.90 - 0.85 - 0.80 - 0.75 - 0.70 - 0.65]$.

The shear capacity V_R was defined in accordance with the three proposed formulations taking into account the variability of the BRV. Provided that no flexural cracking occurred at the shear critical cross section near the end region of the girder with residual prestressing still providing significant contribution, the uncracked resisting mechanism ($V_{R,U}$) was considered to provide shear peak resistance. Under this assumption, the parameter ξ_V was introduced to simulate different shear capacity scenarios:

$$V_R(\xi_V) = \xi_V \cdot V_{R,U}$$

with $\xi_V = [1.40 - 1.30 - 1.20 - 1.10 - 1.00 - 0.95 - 0.90 - 0.85 - 0.80]$.

For cracking limit state, the following values of the parameter ξ_{CR} were considered:

$$\xi_{CR} = [1.00 - 0.95 - 0.90 - 0.85 - 0.80 - 0.75 - 0.70 - 0.65]$$

Table 2
Geometrical properties.

Geometrical property	Symbol	Unit	Value	Notes
Span Length	L	m	42	Simple supported beam
Carriageway Width	w	m	8.9	
Total Deck Height	H	m	3.3	Beam + Slab
Effective Depth of Reinforcing Steel	d_s	mm	3260	$H - c_s$
Effective Depth of Prestressing Steel	d_{sp}	mm	3135	$H - c_{sp}$
Design Prestressing Steel Area	A_{sp}	mm^2	7740	80 strands of 7 wires 1/2"
ETD† from the Bottom at Mid-Span	c_{sp}	mm	165	
ETD† from the Bottom at the Shear-Critical Section	c_{spc}	mm	1100	At $d = H$ from the support
Equivalent Tendon Inclination at Support	ψ	°	3.8	
Undamaged (Design) Reinforcing Steel Area	A_s	mm^2	2670	6Φ10 + 7Φ20
Mid-Span Centroid Cover of Reinforcing Steel	c_s	mm	40	
Stirrups Area	A_{sw}	mm^2	100	2Φ8
Stirrups Distance	s	mm	290	
† Equivalent Tendon Distance				

4.4. Permanent Load

A uniformly distributed load $q_G = 52kN/m$ was considered based on original drawings and visual inspections to model deck self-weight ($q_{SW} = 43kN/m$) and non-structural components ($q_{NS} = 9kN/m$).

4.5. Traffic load

Bending moments and shear forces due to traffic load were computed for the edge girder, whose transversal influence line for a unitary vertical force moving along the bridge deck cross-section is depicted in Fig. 6. To compute the Eurocode characteristic traffic load effect, LM1 was implemented as the resultant of two partial systems, namely tandems ($Q_{1k} = 300kN$; $Q_{2k} = 200kN$) and uniformly distributed loads ($q_{1k} = 9kN/m^2$; $q_{2k} = 2,5kN/m^2$) for the first and the secondary notional lanes both 3 m wide. The remaining area providing an incremental load effect was loaded with $q_{rk} = 2,5kN/m^2$. The transverse load configuration was the same for both bending moment and shear effects (Fig. 6).

Primary $k^{(1)}$ and secondary $k^{(2)}$ stiffnesses were computed and a corrective factor $\epsilon = 0.859$ was obtained considering the actual deck geometry, simply supported scheme and section positioned at $L/2$, where $\varphi(x)$ is maximum. For this reason, the correction factor was applied for the analysis of bending moment only. In terms of longitudinal position of LM1, the sections with the highest bending moment and shear resulting in the lowest CDRs are located at mid-span ($x = L/2$) and near the support ($x = d$), respectively (Fig. 7 and Fig. 8).

The control and critical section for shear was set at a distance d from the support. For loads applied on the upper side within a distance $0.5d \leq a_v \leq 2d$ from the support, the Eurocode [15] allows to reduce the shear force by $\beta = a_v/2d < 1$, limiting the value $a_v = 0.5d$ for $a_v \leq 0.5d$. The maximum shear for the control section was obtained when the closest tandem axle is acting at a distance equal to $a_v = 2d$.

The characteristic traffic load effects due to LM1 are the following:

- $M_k^{LM1} = 10.6\ MNm$
- $V_k^{LM1} = 910\ kN$

4.6. Proof loads

Magnification factors α of LM1 effects were selected in the following range to investigate the impact of different magnitudes of the PLT:

$\alpha = [0.8 - 0.9 - 1.0 - 1.1 - 1.2 - 1.3]$

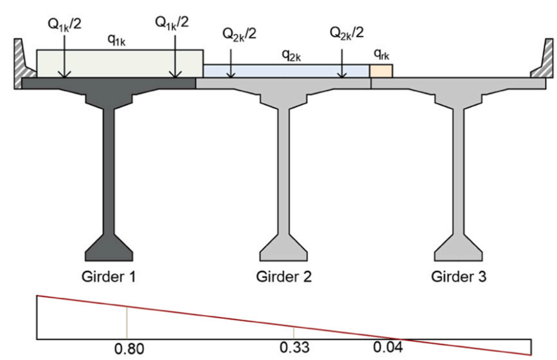

Fig. 6. Transversal Position of LM1 and Girder 1 Influence Line.

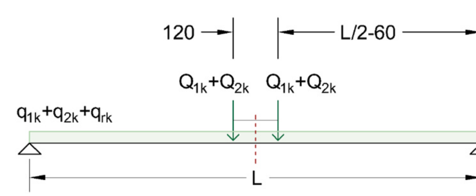

Fig. 7. Longitudinal Position of LM1 for max bending moment at midspan (dimensions in cm).

Table 3
Mechanical random variables.

Material	Variables	Symbol	Unit	Mean	CoV	RV Model
PS	Conventional Yielding Strength	$f_{p,01}$	MPa	1645 [a,b,c]	2.5 % [b,c]	Normal[b]
PS	Initial Stress	σ_{0p}	MPa	1355[a]	3.0 %	Normal
PS	Percentage of Prestressing Losses (t = ∞)	Δl	-	0.25[a]	10.0 %	Normal[b]
RS	Yield Strength	f_y	MPa	500 [a,b]	6.0 %[b]	Normal[b]
C	Compressive Strength	f_c	MPa	35.6[d]	20 %	LogNormal
C	Tensile Strength	f_{ct}	MPa	2.7[e]	20 %	LogNormal

[a] - Original reports
[b] - Joint Committee on Structural Safety (2000) [24]
[c] - Federation Internationale de la Prècontrainte (1976) [17]
[d] - Laboratory experimental tests
[e] - Indirect relationship with f_{cm} based on EN 1992–1–1 (2004) [15] and Italian Ministry of Infrastructures and Transportation. (2018) [23]

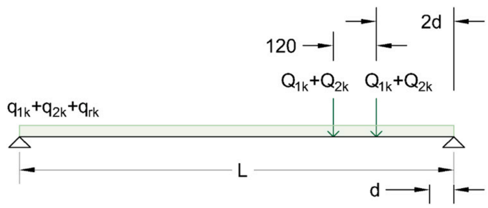

Fig. 8. Longitudinal Position of LM1 for max shear at support (dimensions in cm).

4.7. Model Uncertainties

MUs are summarized in Table 4. The use of a lognormal distribution for MU is supported by relevant literature, including PMC [24] and fib bulletin 80 [18], due to its appropriateness for positive and multiplicative random variables. The parameters for load effect and flexural resistance MUs were assumed as per [18]. Due to the lack of specific references for the adopted shear-tension capacity model governing girder shear resistance, MU suggested in [18] for tensile force in the web was assumed while increasing corresponding COV from 5 % to 10 %. Proof load CoV_{PL_α} is discussed in Section 3.4.

4.8. Random variables and limit states

Random variables considered for flexure, shear and cracking limit states are shown in Fig. 9 and Fig. 10. It should be noted that regarding shear the condition $V_R = V_{R,U}$ for the section under consideration ($x = d$) was attained for all the realizations thus providing shear tension failure as governing mechanism due to low transverse reinforcement ratio.

4.9. Capacity-demand ratios

Partial safety factors (Table 5) were adopted in accordance with Eurocodes [13]:

Table 6, Table 7 and Table 8 show the different CDRs adopted in the following analyses, according to Eqs. 17 to 19. It can be noted that while actual bending capacity would be satisfactory, shear CDR was found to be equal to 0.79 thus providing substandard safety levels of the bridge. This outcome was determined according to PSFM and could be expected as the bridge was designed with low transverse reinforcement ratio and a different traffic load model than LM1(Table 9).

4.10. Results of sensitivity analysis

In this section the results are presented considering different values of CDRs, CoV_{TL} and α in order to investigate the impact of the PLT on this type of bridge deck. Based on prior information and modelling, 50-year values of β_{before} are reported in Fig. 11 for three different values of CoV_{TL}. In the same figure, three threshold values of the reliability index are

Table 4
Model uncertainties.

Random Variables	Symbol	Unit	Mean	CoV	RV Model
Flexural Resistance Model Uncertainty	$\theta_{R,F}$	-	1.00[b]	5 %[b]	LogNormal[a, b]
Shear Resistance Model Uncertainty	$\theta_{R,S}$	-	1.00[b]	10 %[c]	LogNormal[b]
Load Effect Uncertainty	θ_E	-	1.00[b]	10 %[b]	LogNormal[a, b]
Proof Load Model Uncertainty	θ_{PL}	-	1.00[c]	5 %[c]	LogNormal[c]

[a] - Joint Committee on Structural Safety (2000) [24]
[b] - Fédération Internationale du Béton (FIB) (2016) [18]
[c] - selected by engineering judgment

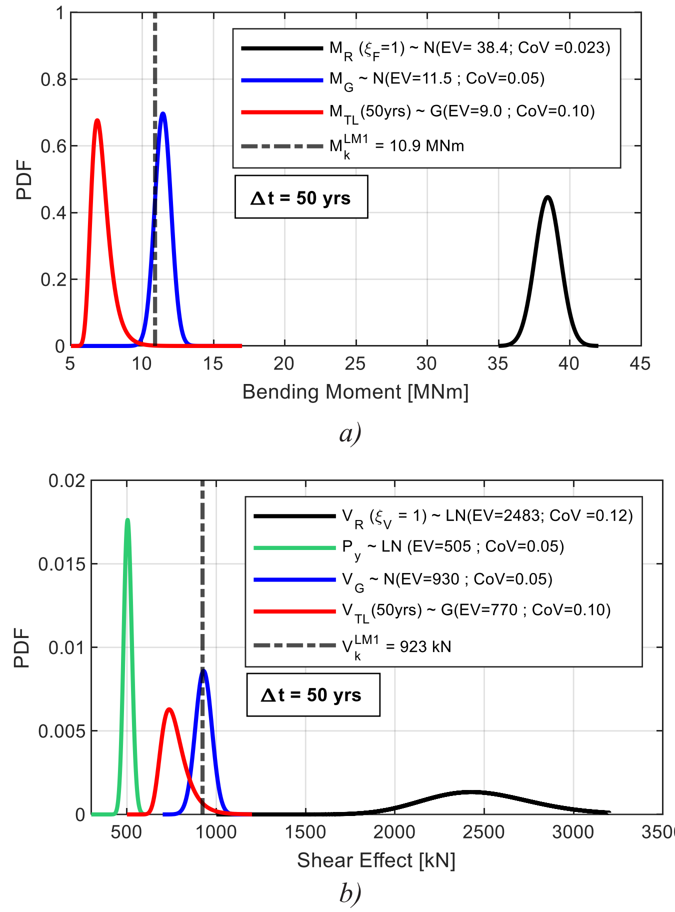

Fig. 9. Demand and Capacity PDFs for (a) Flexural (x = L/2) and (b) Shear (x = d) Limit States.

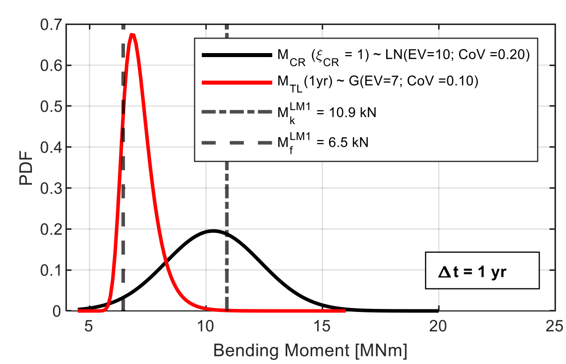

Fig. 10. Demand and Capacity PDFs for Cracking Limit State (x = L/2).

Table 5
Partial safety factors.

Symbol	Value	Object
γ_S	1.15	Steel
γ_C	1.50	Concrete
γ_G	1.35	Dead Load
γ_{TL}	1.35	Traffic Load
γ_P	1.00	Prestressing

Table 6
Flexure CDRs.

ξ_F	**1.00**	0.95	0.90	0.85	0.80	0.75	0.70	0.65
$CDR(\xi_F)$	**1.20**	1.14	1.08	1.02	0.96	0.90	0.84	0.78

Table 7
Shear CDRs.

ξ_V	1.40	1.30	1.20	1.10	**1.00**	0.95	0.90	0.85	0.80
$CDR(\xi_V)$	1.10	1.03	0.95	0.87	**0.79**	0.75	0.71	0.67	0.63

Table 8
Cracking CDRs.

ξ_{CR}	**1.00**	0.95	0.90	0.85	0.80	0.75	0.70	0.65
$CDR(\xi_{CR})$	**1.93**	1.83	1.73	1.64	1.54	1.45	1.35	1.25

shown, i.e. β_0 for assessment ($CC2 = 2.3$; $CC3 = 2.8$) and β_{up} in case of structural upgrading ($CC3 = 3.8$). This comparison provides a straightforward identification of the girder cross sections that exhibit an acceptable safety level, i.e., those cross-sections with a reliability index β exceeding a target value β_{target}. The value β_{target} mainly depends on the bridge safety conditions (e.g., with or without structural upgrading) and on its class of consequences (e.g., CC2 or CC3).

The effect of CoV_{TL} on β_{before} was found to be almost negligible for CDRs around unity. However, a high value of CoV_{TL} turns into more conservative results for girders with $CDR > 1.0$. Instead, for sections with $CDR < 1.0$ a lower CoV_{TL} is less favourable to β_{before}. It can be noted that there is an acceptable matching between unitary CDRs and corresponding reliability index, demonstrating the consistency of the models since for $CDR = 1.0$ the value β_{before} falls in a range between 3.5 and 4.8.

Flexural mechanisms with a $CDR \geq 0.95$ would provide adequate safety levels for existing structure (i.e. $\beta_{before} > \beta_0^{CC3}$). Alternatively for shear, resistance estimation based on the prior knowledge of material properties and code formulations seems overly conservative when considering LM1, turning into a $\beta_{before} > \beta_0^{CC3}$ for $CDR \geq 0.70$. This discrepancy could be attributed to a significant underestimation of the actual shear capacity by the shear-tension capacity model. In this regard it is worth to mention that no distress had been inspected at the end regions of the girders.

Table 9
PLT results for shear.

MECHANISM	CDR ($\xi_i = 1$)	CoV_{TL}	β_{before}	β_{after} ($\alpha = 1$)	$\frac{\Delta\beta}{\beta_{before}}$[%]	$P^u_{f,during}$ ($\alpha = 1$)
		5 %	3.48	3.60	**3 %**	
SHEAR	0.79	10 %	3.57	3.67	**3 %**	$4.5{\cdot}10^{-4}$
		15 %	3.54	3.60	**2 %**	

Fig. 12 and Fig. 13 illustrate the β_{after} indexes for different PLs and two CoV_{TL}, confirming that girders with adequate safety levels (i.e. $CDR > 1.0$) do not undergo significant benefits from PLT ($\Delta\beta < 0.5$). Conversely, structures with a CDR less than or close to 1.0 show more notable benefits, thus suggesting for those structures PLT as a potential alternative to PSFM. It can be inferred that after a PLT, depending on the selected value of α, sections with a given CDR could achieve the performance level prescribed in terms of β_{target}. Alternatively, once a CDR is known and β_{target} has been set, the design value of α can be calculated accordingly for a PLT.

To quantify the benefit of the PLT, the parameter $\Delta\beta$ was defined as:

$$\Delta\beta = \beta_{after} - \beta_{before}$$

and is shown in Fig. 14 and Fig. 15. Even if cases with lower values of CDR and higher value of α would turn into a reliability increase as high as 2.0 (i.e. failure probability before and after could differ by two order of magnitude), it can be noted that a reliability improvement of approximately 1.0 for flexure and 0.5 for shear would be feasible considering the PLT when also $P^u_{f,during} < P_{f,\max}$ could be tolerable (Fig. 16).

Fig. 16 shows the $P^u_{f,during}$ for bending and shear during the PLT without being informed by the success of the previous load step. Given an arbitrary threshold of the probability of failure during the test $P_{f,\max}$ equal to 0.01 [39], it can be found that higher α values result in higher probability of causing failure to the structure, thus PLT becomes unacceptable for CDRs lower than certain values. When combining potential CDR–α values in Fig. 16 practitioners can estimate the order of magnitude of the failure probability and adopt specific load protocols with discrete load steps and specific monitoring systems accordingly. For the case study bridge, for $\alpha = 1$, $P^u_{f,during}$ was found to be $4.5{\cdot}10^{-4}$ for shear and lower than 10^{-6} for flexure.

For cracking limit state, Fig. 17a shows the unconditional probability of cracking the bridge (P^u_{CR}) for different values of α and CDR, while Fig. 17b presents the conditioned probability of cracking the bridge through the up-dated information on actual resistance given by the successful application of the previous loading step (P^c_{CR}) for the case of $CDR(\xi_{CR}) = 1.93$ and $CoV_{PL} = 5\%$. Considering an increasing number of loading steps (N_{LS}) for a given PL_α it is possible to observe how real-time resistance variable updating allows to reduce the probability of cracking significantly, i.e. from $P^u_{CR} = 0.6$ to $P^c_{CR} = 0.1$ for N_{LS} increasing from 4 to 1000, respectively. This outcome demonstrates how multi-step proof loading could be beneficial to reduce the probability of damaging the bridge within acceptable values. Additional benefit is provided by monitoring systems aimed at informing the successful implementation

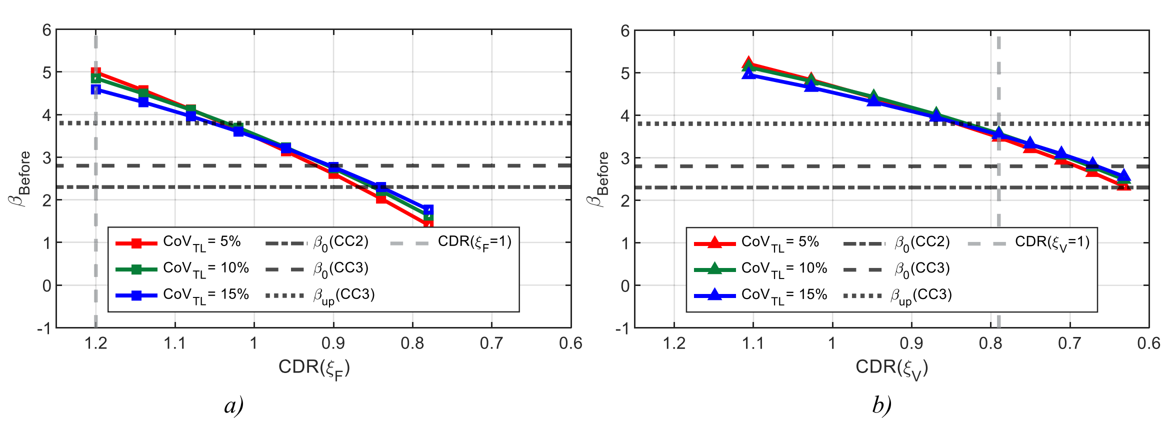

Fig. 11. Flexure (a) and shear (b) β_{Before} for different CoV_{TL} ($\Delta t = 50$yr).

of the previous load step [12] thus overcoming one of the main limitations of the PLT.

4.11. Proof load test

A static load test was performed (Fig. 18) on the case study assuming α=1, imposing the load effects $M_k^{LM1} = 10.6MNm$ and $V_k^{LM1} = 910kN$. It was performed with a total of eight dump trucks with a gross weight of 42 ton each. The target load was imposed in four different steps (two per each step in the order of numbered trucks) and, after each step, a 10-minute time interval was necessary to measure steady-state deflections. In Fig. 19 the layout of the trucks position adopted during the test is shown, as well as the measurement points for monitoring vertical deflections through displacement transducers (11 dial gauges) installed beneath the girders at red points in Fig. 19. The test was run in a single day, while in previous day instrumentation layout was installed. During the test on the deck the traffic was closed and diverted to the opposite deck resulting in limited impact on the serviceability of the highway.

In Fig. 20, the transversal deck deflection profile is reported for the four load steps actually performed during the proof load test (25% –50% –75% –100% of total trucks'weight) before imposing target value with $\alpha = 1$. It can be noted that the three girders were perfectly aligned during all steps thus validating the rigid body motion in torsion as assumed in the closed form analysis of the deck cross section under traffic loads.

For the mid-span cross section with a flexural $CDR = 1.2$, the performed PLT turns into negligible effects in terms of increased reliability.

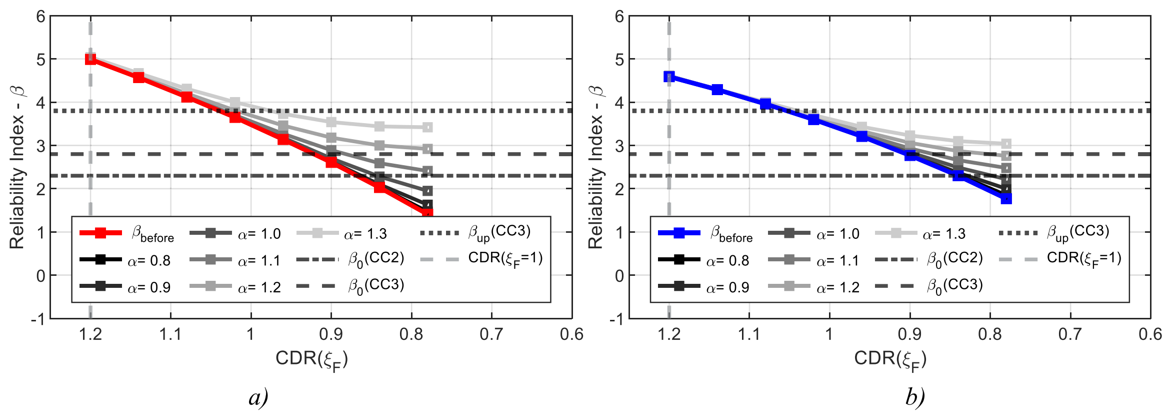

Fig. 12. Flexural mechanism β_{Before} vs β_{After} for different CoV of traffic action ($\Delta t = 50yrs$): a) 5 %; b) 15 %.

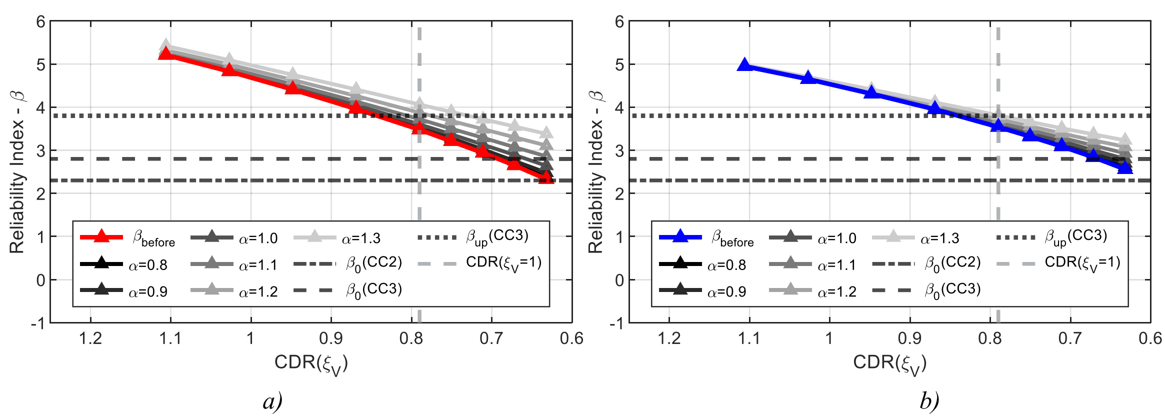

Fig. 13. Shear mechanism β_{Before} vs β_{After} for different CoV of traffic action ($\Delta t = 50yrs$): a) 5 %; b) 15 %.

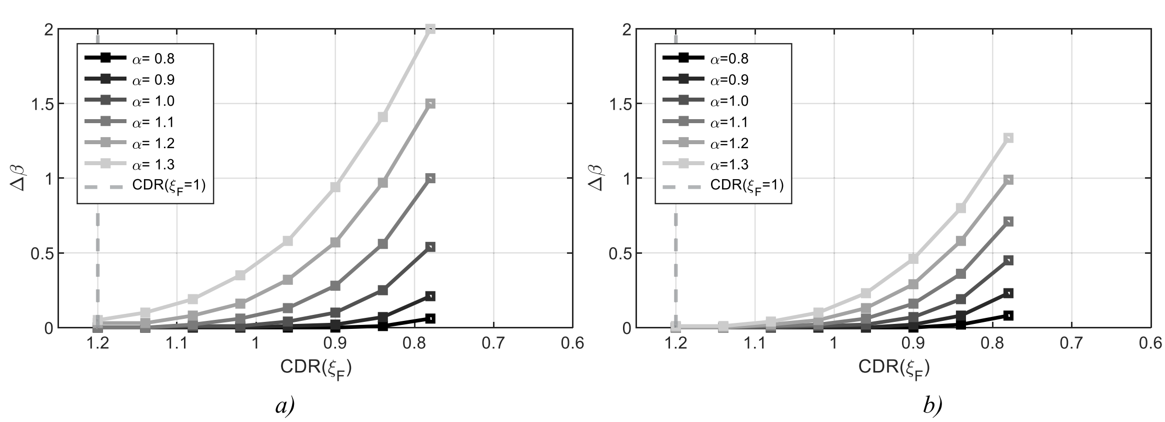

Fig. 14. Flexure mechanism $\Delta\beta$ for different CoV ($\Delta t = 50yrs$): a) 5 %; b) 15 %.

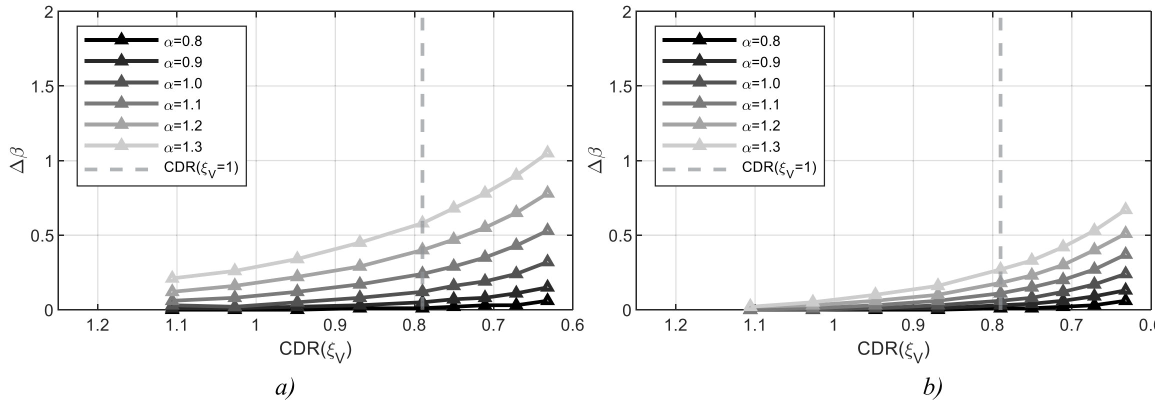

Fig. 15. Shear mechanism $\Delta\beta$ for different CoV ($\Delta t = 50yrs$): a) 5 %; b) 15 %.

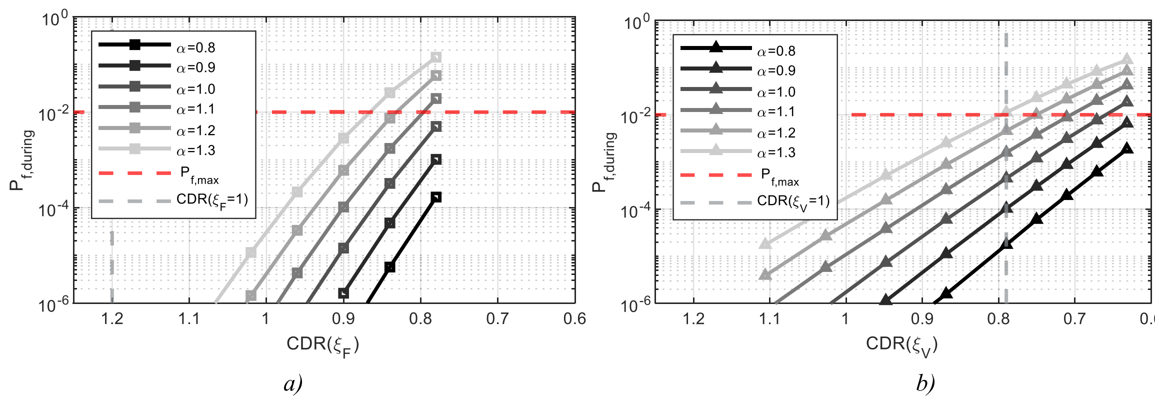

Fig. 16. $P^{u}_{f,during}$ for flexure (a) and shear (b).

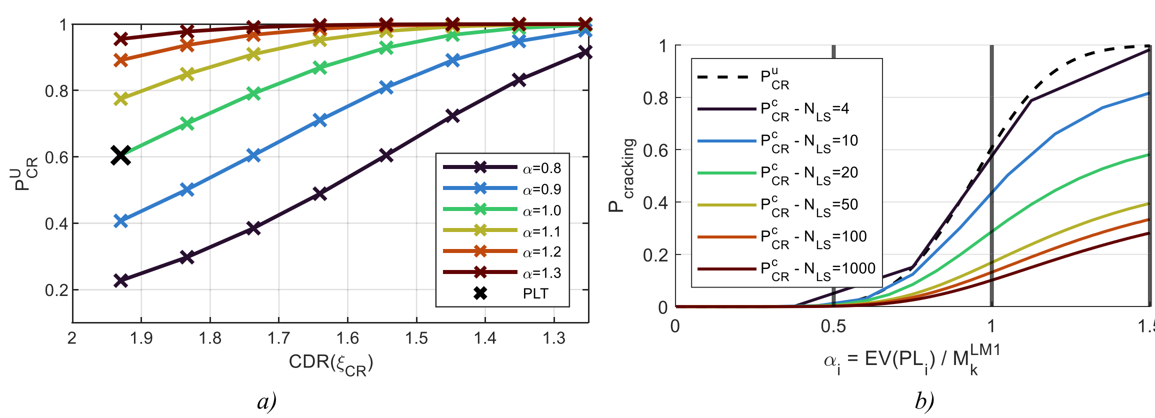

Fig. 17. Cracking limit state: a) P^{u}_{CR}; b) P^{c}_{CR} compared to P^{u}_{CR} as function of N_{LS} for $CDR(\xi_{CR}) = 1.93$ and $CoV_{PL} = 0.05$.

Even if a similar consideration can be derived for the shear mechanism having $CDR = 0.79$ where the benefit from the load test is limited to around 3% in the increase of the reliability index, the PLT provided adequate safety levels of the bridge resulting in $\beta_{after} > 2.8$. This result demonstrated that PLT has a positive effect on the prior estimation of the structural reliability ($\beta_{after} > \beta_{before}$) although its impact is limited in some scenarios. PLT could be a valuable alternative to reliability analysis especially when capacity models are overly conservative and may result in underestimated safety levels according to PSFM.

With respect to cracking ($CDR = 1.93$) and shear tension mechanism the PLT enabled a significant reduction of mechanical uncertainties related to concrete tensile strength and residual prestressing with $\beta_{after} > 2.8$, thus avoiding costly strengthening interventions on the whole bridge consisting of 126 girders. While the predicted unconditioned probability of cracking was relatively high ($P^{u}_{CR} = 0.6$), the load test was performed in four load steps without any observed damage, consequently confirming a potential underestimation of concrete tensile strength and/or residual prestressing.

5. Discussion

The findings of the present study contribute to highlight the positive impact of PLT on the safety assessment of existing PC I-girder-type bridges which is a very common bridge archetype in some countries like Italy.

PLT demonstrated its potential for resisting mechanisms governed by

Fig. 18. Execution of the PLT on the case study bridge.

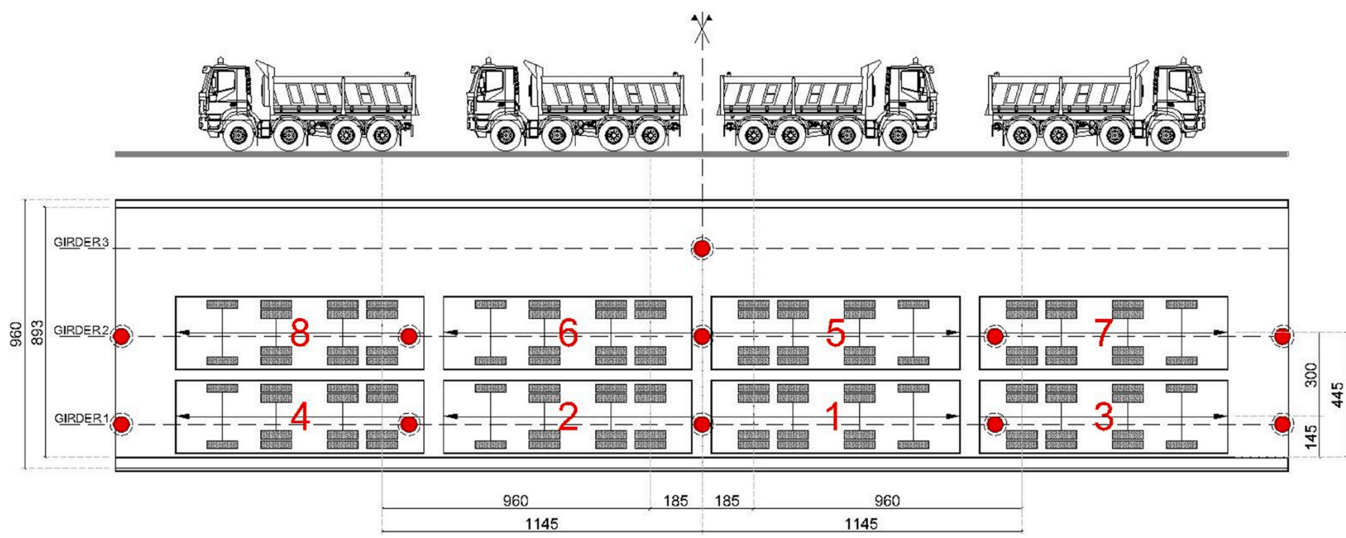

Fig. 19. Layout of the truck and displacement transducers position (red dots) (dimensions in cm).

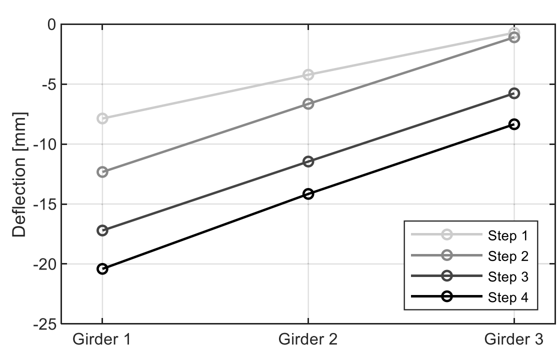

Fig. 20. Transverse deck deflection at midspan.

higher level of conservatism and uncertainties: while available formulations underestimated actual shear resistance of the case study, PLT turned into adequate safety levels. The case study addressed that a reliability-based structural analysis could provide satisfactory safety levels (i.e. $\beta_{before} > \beta_{target}$), suggesting that PLT might be apparently redundant or even unnecessary. This apparent redundancy of PLT holds only when the basic assumptions on material and geometrical properties or multi-hazard conditions are properly defined in terms of accuracy and limited uncertainty. In practice, PLT can provide valuable empirical information on the minimum proof resistance taking into account actual bridge conditions which in a desk-study analysis could only be estimated to the best of someone's knowledge, for instance in terms of section shear strength, concrete tensile strength, residual prestress level, residual service life, impact of corrosion or deteriorations effects. Additionally, since decision-making is dependent on different goals, available tools, time, and budget, such a conclusion would be simplistic and based purely on analytical considerations, requiring a broader perspective to account for the benefits of PLT. When considering common practice in structural engineering a fully probabilistic analysis is outside of professionals' expertise and a PLT proves to be less expensive both in terms of costs and time. This consideration is underpinned considering that a reliability analysis usually requires not only higher-level professional expertise but often the preliminary design and execution of extensive investigations, with inherently increase in time and costs requirements. While conducting a reliability analysis in common practice could be challenging, in some countries like Italy where a high number of roadway bridges have to be assessed in the coming years, PLT can be feasible, straightforward to implement and well accepted by engineering community. Additionally, PLT is a way to collect valuable field data, validate numerical models and update probabilistic models with measurement data. Furthermore, where timely decisions on bridge safety are needed PLT represents a time-effective alternative to reliability analysis.

The methodology presented herein represents a further development of PLT compared to the state-of-the-art. Obtained results align well with previous and seminal studies [27,35] where the concept that proof loading leads to an increase in structural reliability is postulated. The magnitude of the benefit provided by the PLT mainly depends on the level of uncertainty about the BRVs and the limitations of conventional methods.

Target proof-load factors, as previously defined in [7,11], are considered to demonstrate that a bridge successfully reaching a specified test load achieves a target reliability for a pre-defined load level. The same approach is retained in present study where the empirical WIM-based traffic model is replaced with a code-consistent traffic load formulation based on Eurocode 1 characteristic load LM1. This provides an alternative method to WIM-based models such as those presented in [7]. This study confirms previous results from [7] corroborating the concept that in order to be effective target loads in PLT should be higher than actual traffic loads. Along the same line, [39] showed that PLT effectiveness requires accepting a certain probability of failure during load testing based on prior information. Recently in [12] considering potential damage during PLT, the authors proposed a methodology to quantify both the probability of cracking and severe damage during the load test. Based on previous laboratory-based conditioning and real-time monitoring system adopted in situ, the methodology advanced in [12] shows that cracking probability significantly decreases as the number of controlled loading steps increases.

Stop criteria represent a valuable tool to prevent damage and to warn for imminent danger of collapse, combining serviceability and ultimate limit states [19]. Finally, assuming the failure probability during the test bounded to acceptable values, the benefits of PLT involve the extension of the service life of existing bridges combined with economic and environmental sustainability.

6. Conclusions

Proof load testing (PLT) can be a highly effective empirical method for updating the safety of existing bridges, particularly when knowledge about the structure is limited or in the presence of substantial uncertainties related to structural system behavior and resistance estimation (including material variability, model uncertainty, boundary conditions). Quantitatively, for values CDR $\in$ [0.7–1.0], which are common for existing bridges, proof-load testing can led to a significant increase in reliability index assuming $\alpha \in$ [1.1–1.3]. In some cases, it was demonstrated that after PLT the value of β almost increased by two thus reducing the corresponding probability of failure by two orders of magnitude. This benefit in terms of reduced probability of failure becomes larger as the CDR decreases or uncertainties associated with considered failure mechanism become higher as in the case of shear mechanism. Results in the CDR $-\beta_{before}$ plots showed a rightward shift of the shear-reliability curves compared to flexure-reliability ones, highlighting the higher conservatism of the formers turning into lower CDR value for a fixed β compared to the latters. Hence, with a CDR in the range of [0.65–0.90], an amplification factor $\alpha = 1.1$ could provide a posterior reliability between 2.8 and 3.8 for shear. In case of flexure, when CDR is in the range [0.8–1.0], the same target reliability is achieved with a minimum value of α equal to 1.2.

Specific considerations should be made regarding damage prevention during the test, target PLT and reliability levels both during and after the test, as well as its overall feasibility. This paper presented a study on the positive impact of PLT on existing PC I-girder bridge decks based on the Eurocode-conforming traffic load model and different capacity levels of the main girders.

The present study investigated the proof load effects based on reliability analysis taking into account the probability of damaging the structure during the test. The results demonstrated that in case of lower safety levels, the reliability of the bridge given survival after the PLT would be significantly increased, but the high failure probability during the test may result in unacceptable risk for the managing agency. A real case study bridge demonstrated the positive outcome of the PLT in achieving a satisfactory reliability level for the shear mechanism ($\beta_{after} = 3.60$) thus avoiding expensive strengthening interventions.

The results highlight that higher proof loads are quite dangerous during the test but significantly enhance the posterior reliability once the test is successfully completed thus highlighting the role of monitoring to reduce uncertainties. A significant improvement in the reduction of the failure probability during the test is offered by the definition of a step-by-step loading protocol, discretizing the loading target load in such a way that a single load step can be conceived as a proof load that can update the following step estimated probability of exceeding the limit state under consideration. In order to mitigate this risk, it was proven that a target proof-load attained with at least 4 and up to 50 discrete steps can significantly reduce the cracking probability during the test.

Therefore, it was shown that, based on CDR, the practitioners can estimate the reliability index after a successful test and design target load accounting for combined benefit and risk. In further studies, the current results will be compared to different case studies trying to develop a general framework for PLT of the considered bridge class.

The proposed methodology will be applied to additional I-type bridges in order to provide proper validation and define a practical tool for safety assessment of existing bridges through PLT. In future studies, the load history of the bridge will be also taken into account to reduce prior uncertainties. A risk assessment of the proof load based on direct and indirect estimation of losses will also be developed to define acceptable levels of the proof load, exploring the impact of lack of knowledge about resistance on the PLT benefit.

CRediT authorship contribution statement

Casas Joan Ramon: Writing – original draft, Visualization, Validation, Supervision, Methodology, Investigation, Conceptualization. **Daniele Losanno:** Writing – original draft, Visualization, Validation, Supervision, Project administration, Methodology, Investigation, Funding acquisition, Conceptualization. **Lantsoght Eva Olivia Leontien:** Writing – original draft, Visualization, Validation, Supervision, Methodology, Investigation, Conceptualization. **Gianmarco Addonizio:** Writing – original draft, Visualization, Software, Methodology, Investigation, Formal analysis, Data curation, Conceptualization.

Declaration of Competing Interest

The authors declare that they have no known competing financial interests or personal relationships that could have appeared to influence the work reported in this paper.

Acknowledgements

This study was developed within the CSLLP-ReLUIS project funded by the Italian High Council of Public Works.

Data availability

Data will be made available on request.

References

[1] AASHTO. *Manual for Bridge Evaluation* (MBE). Washington, D.C.: American Association of State Highway and Transportation Officials; 2011.

[2] Agredo Chávez A, Gonzalez-Libreros J, Wang C, Capacci L, Biondini F, Elfgren L, Sas G. Assessment of residual prestress in existing concrete bridges: the Kalix bridge. Eng Struct 2024;311:118194. https://doi.org/10.1016/j.engstruct.2024.118194.

[3] Anay R, Cortez TM, Jáuregui DV, ElBatanouny MK, Ziehl P. On-site acoustic-emission monitoring for assessment of a prestressed concrete double-tee-beambridge without plans. J Perform Constr Facil 2015;34(3). https://doi.org/10.1061/(ASCE)CF.1943-5509.0001440.

[4] ANSFISA. (2022). *Relazione annuale sulla sicurezza delle ferrovie e delle instrastrutture stradali e autostradali.* Agenzia Nazionale per la Sicurezza delle Ferrovie e delle Infrastrutture Stradali ed Autostradali, Roma.

[5] Bell, B., Bien, J., Cremona, C., Feltrin, G., Jensen, J.S., Kiviluoma, R., … Elfgren, L. (2023). Sustainable Bridges – Past and Future. Reflections on a European Project 2003 – 2007. *IABSE Congress 2023 New Delhi*, 690-698.

[6] Calvi GM, Moratti M, O'Reilly GJ, Scattarreggia N, Monteiro R, Malomo D, Pinho R. Once upon a time in Italy: the tale of the morandi bridge. Struct Eng Int 2019;29:*1–20*. https://doi.org/10.1080/10168664.2018.1558033.

[7] Casas JR, Gómez JD. Load rating of highway bridges by proof-loading. KSCE J Civ Eng 2013;17:*556–67*. https://doi.org/10.1007/s12205-013-0007-8.

[8] Cavaco ES, Neves LA, Casas JR. On the robustness to corrosion in the life cycle assessment of an existing reinforced concrete bridge. Struct Infrastruct Eng 2018; 14(2):1–14. https://doi.org/10.1080/15732479.2017.1333128.

[9] Cervantes E, Matos J, Lantsoght E. Infraestrutura de pontes no Equador: desafios e soluções. Rev De Ativos De Eng 2024. https://doi.org/10.29073/rae.v2i2.927.

[10] Cosenza E, Losanno D. Assessment of existing reinforced-concrete bridges under road-traffic loads according to the new Italian guidelines. Struct Concr 2021;22: 2868–81. https://doi.org/10.1002/suco.202100147.

[11] de Vries R, Lantsoght E, Steenbergen RN. Proof load testing method by the american association of state highway and transportation officials and suggestions for improvement. J Transp Res Rec 2023;2677(11):*245–57*. https://doi.org/10.1177/03611981231165026.

[12] de Vries R, Lantsoght E, Steenbergen R, Hendriks M, Naaktgeboren M. Structural reliability updating on the basis of proof load testing and monitoring data. Eng Struct 2025;330:119863. https://doi.org/10.1016/j.engstruct.2025.119863.

[13] EN 1990 (2002): Eurocode - Basis of structural design [Authority: The European Union Per Regulation 305/2011, Directive 98/34/EC, Directive 2004/18/EC].

[14] EN 1991-2 (2003): Eurocode 1: Actions on structures - Part 2: Traffic loads on bridges [Authority: The European Union Per Regulation 305/2011, Directive 98/34/EC, Directive 2004/18/EC].

[15] EN 1992-1-1 (2004): Eurocode 2: Design of concrete structures - Part 1-1: General rules and rules for buildings [Authority: The European Union Per Regulation 305/2011, Directive 98/34/EC, Directive 2004/18/EC].

[16] European Commission. (2009). *ARCHES D08: Recommendation on the use of results of monitoring on bridge safety assessment and maintenance - Annex A_ Recommendations on bridge traffic load monitoring. Final Report.* ⟨http://arches.fehrl.org/⟩.

[17] Federation Internationale de la Prècontrainte. (1976). *Report on Prestressing Steel: 1. Types and properties* .

[18] Fédération Internationale du Béton (FIB). (2016). *Bullettin 80 - Partial factor methods for existing concrete structures.* ISBN: 978-2-88394-120-5.

[19] Garnica, G.Z., Lantsoght, E., Yang, Y., & Hendriks, M. (2024). Shear stop criteria for reinforced concrete slab strips. *Bridge Maintenance, Safety, Management, Digitalization and Sustainability.* Copenhagen. https://doi.org/10.1201/9781003483755-36.

[20] Hambly E. Bridge Deck Behaviour. Taylor & Francis; 1991. https://doi.org/10.1201/9781482267167.

[21] International Federation for Structural Concrete (fib). (2020). *Model Code for Concrete Structures* . Lausanne. ISBN: 978-2-88394-175-5.

[22] Italian High Council of Public Works. (2020). *Linee guida per la classificazione e gestione del rischio, la valutazione della sicurezza ed il monitoraggio dei ponti esistenti.* Rome, Italy.

[23] Italian Ministry of Infrastructures and Transportation. (2018). DM 17/01/2018. Aggiornamento delle "Norme tecniche per le costruzioni'. Rome, Italy.

[24] Joint Committee on Structural Safety. (2000). *JCSS Probabilistic Model Code.* ISBN 978-3-909386-79-6.

[25] Lantsoght EO. Assessment of existing concrete bridges by load testing: barriers to code implementation and proposed solutions. Struct Infrastruct Eng 2023;20: *1002–14*. https://doi.org/10.1080/15732479.2023.2264825.

[26] Lichtenstein A. Bridge rating through nondestructive load testing. NCHRP 1993;12 (13):*28* (A).

[27] Lin TS, Nowak AS. Proof loading and structural reliability. Reliab Eng 1984;8(2): *85–100*. https://doi.org/10.1016/0143-8174(84)90057-X.

[28] Melchers, R.E., & Beck, A.T. (2018). *Structural Reliability Analysis and Prediction.* Wiley. ISBN: 9781119265993.

[29] Miluccio G, Losanno D, Parisi F, Cosenza E. Fragility analysis of existing prestressed concrete bridges under traffic load according to new Italian guidelines. Struct Concr 2021;24(1):*1053–69*. https://doi.org/10.1002/suco.202200158.

[30] Miluccio G, Losanno D, Parisi F, Cosenza E. Traffic-load fragility models for prestressed concrete girder decks of existing Italian highway bridges. Eng Struct 2021;249(3):113367. https://doi.org/10.1016/j.engstruct.2021.113367.

[31] Pinto P, Franchin P. Issues in the Upgrade of Italian Highway Structures. J Earthq Eng 2010;14(8):*1221–52*. https://doi.org/10.1080/13632461003649970.

[32] Raithel A. Ponti a travata. Napoli: Liguori Editore; 1978.

[33] I.M. SAFE. (2021). *Actual and future context of transport infrastructure monitoring and maintenance - EC Project IM SAFE, Grant agreement No 958171.* https://doi.org/10.3030/958171.

[34] Shenton HW, Chajes J, M, Huang J. Load rating of bridges without plans. J Perform Constr Facil 2007:*298–309*. https://doi.org/10.1061/41130(369)28.

[35] Spaethe G. Die Beeinflussung del Sicherheit eines Tragwerkes durch Probebelastung. Bauingenieur; 1994.

[36] The MathWorks Inc. (2023). MATLAB R2023b. Natick, Massachusetts.

[37] Transportation Research Board. Manual for Bridge Rating Through Load Testing, 234; 1998. ⟨http://onlinepubs.trb.org/onlinepubs/nchrp/nchrp_rrd_234.pdf⟩.

[38] Transportation Research Board. (2019). Primer on Bridge Load Testing (Number E-C257).

[39] Wang C, Zhang H. A probabilistic framework to optimize the target proof load for existing bridges. Innov Infrastruct Solut 2020;5(12). https://doi.org/10.1007/s41062-020-0261-9.